Biol. Cybern. 65, 81–90 (1991)

Biological Cybernetics

A computer based model for realistic simulations of neural networks

I. The single neuron and synaptic interaction

Ö. Ekeberg [1], P. Wallén [2], A. Lansner [1], H. Tråvén [1], L. Brodin [2], and S. Grillner [2]

[1] Department of Numerical Analysis and Computing Science, Royal Institute of Technology, S-100 44 Stockholm, Sweden
[2] Nobel Institute for Neurophysiology, Karolinska Institutet, Box 60400, S-104 01 Stockholm, Sweden

Received June 18, 1990/Accepted in revised form April 9, 1991

Abstract. The use of computer simulations as a neurophysiological tool creates new possibilities to understand complex systems and to test whether a given model can explain experimental findings. Simulations, however, require a detailed specification of the model, including the nerve cell action potential and synaptic transmission. We describe a neuron model of intermediate complexity, with a small number of compartments representing the soma and the dendritic tree, and equipped with Na^+, K^+, Ca^{2+}, and Ca^{2+} dependent K^+ channels. Conductance changes in the different compartments are used to model conventional excitatory and inhibitory synaptic interactions. Voltage dependent NMDA-receptor channels are also included, and influence both the electrical conductance and the inflow of Ca^{2+} ions. This neuron model has been designed for the analysis of neural networks and specifically for the simulation of the network generating locomotion in a simple vertebrate, the lamprey. By assigning experimentally established properties to the simulated cells and their synapses, it has been possible to verify the sufficiency of these properties to account for a number of experimental findings of the network in operation. The model is, however, sufficiently general to be useful for realistic simulation also of other neural systems.

1 Introduction

Mathematical modeling has long been used in neuroscience to study different mechanisms of both single neurons (Hodgkin and Huxley 1952; Frankenhaeuser and Huxley 1964; Wallöe 1968; Kernell and Sjöholm 1972; Rall 1977; Edman et al. 1987a, b) and of systems of neurons (Stein 1965; MacGregor and Oliver 1974; Perkel 1976; Lansner 1982; MacGregor 1987; Mulloney and Perkel 1988; Koch and Segev 1989; Roberts and Tunstall 1990). The analyzing power of mathematical models and computer simulations is well recognized. The complexity of the different models has ranged from relatively simple neurons, merely modeled as input-output devices producing a "spike" output of a certain frequency if a threshold is reached, to highly complex models that incorporate a variety of membrane- and other parameters (biophysical as well as morphological; Holden 1980). Recently, the interest in using computer simulations of realistic neuronal models has markedly increased. Various kinds of neurons and neural systems have been simulated (for review, see Getting 1989). Also, within the computer science field, the interest in neural networks is rapidly growing (Anderson and Rosenfeld 1988; Rumelhart and McClelland 1986; Lippmann 1987; Lansner and Ekeberg 1985, 1989).

In order to fully elucidate the mechanisms of operation of for instance a motor system, we must take into account all available information on different levels, including cellular properties (e.g. pacemaker potentials), synaptic interactions etc. Even with a lot of detailed experimental information at hand, it is difficult to understand the system as a whole. All this information must be put together to evaluate the relative contributions and roles of different factors to the overall operation of the system. To achieve this goal, computer simulations of the system under study, using a model that incorporates the experimentally established parameters, appears as the only feasible way. In general, making a reasonable computer model requires a much more detailed description than formulating a theoretical, conceptual model. The main difference is that the computer model has to be quantitative in all its details, while the conceptual model usually is more qualitative. Further, no parts of the model can be left out as "common knowledge". Every mechanism that significantly influences the operation of the network has to be specified.

In our investigations of the neuronal mechanisms underlying locomotor behavior in vertebrates (Grillner et al. 1987, 1988, 1989, 1991), we have for several years been utilizing the in vitro preparation of the lamprey CNS (Grillner et al. 1987) as a biological model. The interneuronal network responsible for the rhythmical alternating activity during locomotion (swimming) is

located within the spinal cord, and a conceptual model of the segmental pattern-generating circuitry, based on experimentally established neuron types and detailed knowledge of synaptic connections, postsynaptic receptors and membrane properties, has been presented (Grillner et al. 1987, 1991; Buchanan and Grillner 1987).

When trying to assess to what an extent this conceptual model can account for the behavior of the biological system, we were faced with the problem of having to test the relative roles of the various features and properties of the system, i.e. to integrate the large body of experimental data into a testable model system that would correspond approximately to the locomotor system in operation. Thus, we set out to design a computer model; sufficiently detailed to incorporate all experimentally established properties of importance; yet simplified enough to allow simulations of several neurons in a network on available computers within a reasonable time. Also, the degree of complexity of the model had to be chosen so that the simulated output could be readily interpreted and compared to the experimental findings. In our initial modeling studies, it was possible to simulate some aspects of the rhythm-generating capability of the lamprey locomotor network (Grillner et al. 1988, 1989). The present study is the first in a series, describing the computer simulations of the lamprey network in detail, and is focussed upon the modeling of the single neuron and the synaptic transmission. With a network of these model neurons the full range of locomotor activity, including the brainstem control of the segmental network and the influence from sensory feedback signals has been simulated (Grillner et al. 1991 and unpubl.).

2 The single cell model

In the conceptual model, there was no need to take into account the detailed dendritic branching pattern of the different neurons. Therefore, in the single cell model, no attempt was made to describe the detailed morphology. However, to allow for synaptic input at different distances from the soma, a simple representation of the dendritic tree was included. Like in many similar models, the neuron is represented by a set of electrically coupled isopotential compartments. Four such compartments have been used here, one representing the soma and the other three the dendritic tree at various distances from the soma (Fig. 1A). In principle, however, any number of compartments could be used in this model.

The primary state variable in each compartment is the intracellular potential E, which is computed by calculating the ionic currents flowing into and out from the compartment. This includes the passive coupling of the compartments as well as active ion channels of different types.

In this model we have not simulated the actual mechanisms underlying the propagation of the nerve impulse down the axon, but merely the time spent for this propagation. This is based on the assumption that each time the spike initiating part of the cell fires, the action potential travels along the axon with a constant speed and, thus, reaches the terminal after a predetermined delay. In the simulations, this delay is an adjustable parameter for each synapse.

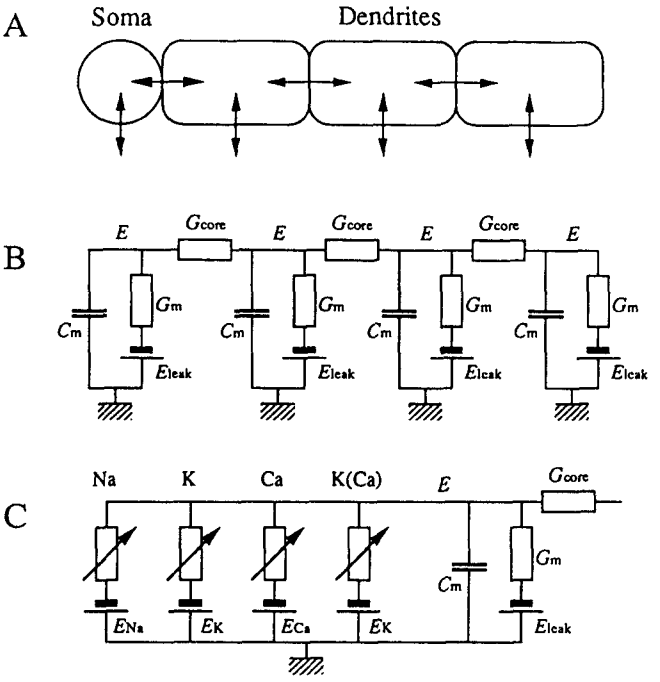

Fig. 1. The model neuron is built around a set of compartments **(A)**. Note that the sizes in the figure do not reflect the actual membrane areas of a typical cell, where the total area of the dendrites can be an order of magnitude larger than that of the soma. The passive properties of the four coupled compartments can be viewed as an equivalent electrical circuit **(B)**. By adding the active ion channels to the model, the electrical equivalent of the soma compartment is extended as in **C**. For explanation of symbols, see text

2.1 Passive properties

Each compartment has a membrane capacitance C_m proportional to the membrane area (Fig. 1B). The potential E is calculated by integrating the currents. This results in a differential equation for each compartment:

$$\frac{dE}{dt} = \frac{(E_{leak} - E)G_m + \sum (E_{comp} - E)G_{core} + I_{channels}}{C_m} \quad (1)$$

First, there is a passive leakage current through the membrane, modeled with a conductance G_m across the membrane. This conductance is set so that an appropriate membrane time constant C_m/G_m is achieved. The equilibrium potential of this current, E_{leak}, is set close to the resting potential of the cell to be simulated, e.g. -70 mV.

Further, the compartments are electrically coupled by conductances G_{core} (Fig. 1B). The summation in the equation above is made over all comparments connected to the compartment in question. In the case of a general dendritic tree structure, this would correspond to one compartment in the proximal direction and

possibly several compartments connected to the distal end. E_{comp} is the potential in the connected compartment. This passive model thus forms a system of coupled ordinary first order differential equations, with one equation for each compartment.

Finally, the $I_{channels}$ term is the currents entering through all the active ion channels into the compartment. How these currents are calculated will be described in the following sections. In the simulations it is also possible to mimic intracellular current injection by simply adding an extra current to the soma compartment. This current can be constant in time to give a tonic stimulation or be varied e.g. to give the effect of a current pulse.

Such a set of coupled ordinary differential equations can be simulated in a computer by the use of a proper numerical method (see below). Given some initial values for the state variables, in this case the electrical potentials in the compartments, the time course of these variables can be computed.

2.2 Action potentials

When a nerve cell is depolarized from the resting membrane potential, different types of voltage gated ion channels will open, provided that the membrane potential reaches a threshold value. Such voltage dependent channels give rise to the action potential, during which sodium channels initially open to bring the membrane potential towards the equilibrium potential for Na^+ ions (around +50 mV). With some delay, voltage dependent potassium channels open, which pulls the membrane potential towards the equilibrium potential for K^+ ions (around −90 mV). The sodium channels have the additional property of closing after a period of depolarization, i.e. they are inactivated, whereas the potassium channels are not (Hodgkin and Huxley 1952; Hille 1984). The potassium channels open slower than sodium channels and are not fast enough to disturb the fast depolarization of the spike. They are, however, faster than the inactivation of sodium channels and therefore constitute the primary factor involved in the rapid repolarization of the spike.

A quantitative model for the sodium and potassium currents was presented by Hodgkin and Huxley as early as 1952, based on a description of the membrane of the squid giant axon. Since then, it has been used for neuronal membranes in general. Here, we have used a modified version of the Hodgkin and Huxley model and adjusted the parameters to match the known characteristics of the real neurons being simulated.

The Hodgkin and Huxley model describes how the mean conductance through the sodium and potassium channels varies with membrane potential and time. It can, however, be interpreted on a single channel level as a two state gate which stochastically changes between an open and a closed state.

The current through sodium channels, entering the soma compartment, is computed as:

$$I_{Na} = (E_{Na} - E_{soma}) G_{Na} m^3 h \tag{2}$$

where E_{Na} is the reversal potential for Na^+, in our simulations set to +50 mV, G_{Na} is the maximum sodium conductance through the membrane and m and h are the degrees of activation and inactivation of the Na^+ channels, respectively.

To be able to fit the model equations to experimental data, some arbitrary exponents were introduced by Hodgkin and Huxley (1952) in their equations. One possible explanation for the need for such exponents is that the channel molecule actually has to perform several state transitions in order to reach an open state (cf. Hille 1984).

The activation of the Na^+ channels is described by a simple differential equation:

$$\frac{dm}{dt} = \alpha_m(1 - m) - \beta_m m \tag{3}$$

where α is the rate by which the channels switch from a closed to an open state and β is the rate for the reverse. α and β depend only on the membrane potential in the soma and are given by the expressions:

$$\alpha_m = \frac{A(E_{soma} - B)}{1 - e^{(B - E_{soma})/C}} \qquad \beta_m = \frac{A(B - E_{soma})}{1 - e^{(E_{soma} - B)/C}} \tag{4}$$

Note that the parameters A, B and C are not necessarily the same for the two expressions.

The inactivation of the Na^+ channels is described by a similar, but not identical, set of equations:

$$\frac{dh}{dt} = \alpha_h(1 - h) - \beta_h h \tag{5}$$

$$\alpha_h = \frac{A(B - E_{soma})}{1 - e^{(E_{soma} - B)/C}} \qquad \beta_h = \frac{A}{1 + e^{(B - E_{soma})/C}} \tag{6}$$

The potassium channels are treated in a similar way, except that an inactivation is not included, resulting in:

$$I_K = (E_K - E_{soma}) G_K n^4 \tag{7}$$

$$\frac{dn}{dt} = \alpha_n(1 - n) - \beta_n n \tag{8}$$

$$\alpha_n = \frac{A(E_{soma} - B)}{1 - e^{(B - E_{soma})/C}} \qquad \beta_n = \frac{A(B - E_{soma})}{1 - e^{(E_{soma} - B)/C}} \tag{9}$$

where n is the degree of activation of the K^+ channels.

We have used an exponent of both four and two in the expression for I_K above (cf. Kernell and Sjöholm 1972). To function properly, the K^+ current has to be delayed not to interrupt the first part of the spike. With an exponent of two, this was difficult to achieve. An exponent of four, however, gives a sufficient delay to postpone the effect of a gradually increasing n.

As with the original Hodgkin and Huxley model, these equations give a model which is capable of producing action potentials with a realistic shape (Fig. 2). With a suitable set of parameters and the addition of calcium dependent potassium channels (see below), it is also possible to get repetitive firing in a realistic frequency range (Fig. 3). The parameters are listed in Table 1.

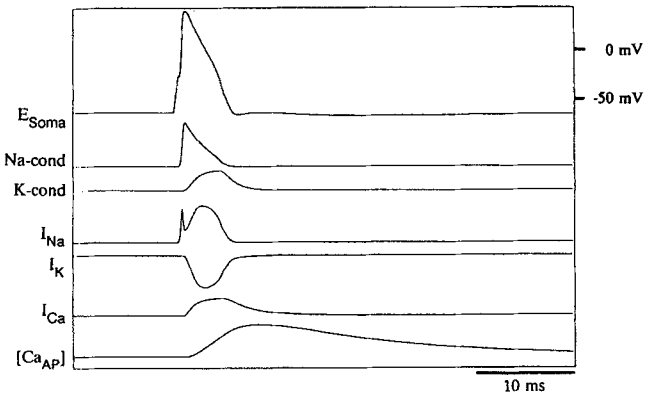

Fig. 2. A simulated action potential with corresponding changes of sodium and potassium conductances, sodium and potassium currents, calcium current, and intracellular calcium concentration. The spike is initiated by a short duration current pulse (0.5 ms)

2.3 Calcium and long lasting AHP

Neurons also have voltage dependent calcium channels (e.g. Tsien 1983; for lamprey, see Hill et al. 1989). Activation of the calcium channels causes an inward, depolarizing flow of Ca^{2+} ions; however, calcium channels generally need a higher degree of depolarization for activation, compared to sodium and potassium channels (cf. Tsien et al. 1988). They open fairly rapidly but close slowly, causing most of the Ca^{2+} to enter after the spike (Fig. 2).

We have chosen to describe the Ca^{2+} channels with a set of equations similar to those used for the Na^+ and K^+ channel activation. Let q denote the degree of activation of the calcium channels:

$$\frac{dq}{dt} = \alpha_q(1-q) - \beta_q q \tag{10}$$

$$\alpha_q = \frac{A(E_{soma} - B)}{1 - e^{(B - E_{soma})/C}} \qquad \beta_q = \frac{A(B - E_{soma})}{1 - e^{(E_{soma} - B)/C}} \tag{11}$$

$$I_{Ca} = (E_{Ca} - E_{soma}) G_{Ca} q^5 \tag{12}$$

The equilibrium potential for the calcium ions, E_{Ca}, was set to +150 mV. An exponent of five, as in the formula above, has earlier been used by e.g. Traub and Llinas (1977) in modeling the calcium current, although they used somewhat different formulae for the rate functions and included an inactivation factor as well. For the sake of our simulations, we have seen no need to include the inactivation and have consequently ignored it to reduce model complexity. The parameters have been adjusted so that the calcium channels open during an action potential and then slowly close (Brodin et al. 1991).

In the types of neurons we are simulating, the depolarizing current resulting from the influx of Ca^{2+} ions can be assumed to be of minor importance, and it has therefore often been ignored in the simulations. The Ca^{2+} ions entering the cell do, however, also influence the electrical properties indirectly by activating calcium dependent ion channels. Such channels are activated by Ca^{2+} ions present on the inside of the cell membrane. This indirect action of Ca^{2+} is of considerable importance in lamprey neurons as well as in many other types of neurons and, thus, included in the model.

It seems reasonable to assume that, following an action potential, opening of the Ca^{2+} channels will cause a transient increase of the intracellular Ca^{2+} concentration primarily in the vicinity of the Ca^{2+} channels. In the model, this is represented by a Ca^{2+} ion pool which we will denote the Ca_{AP}-pool. The ions enter the Ca_{AP}-pool through the calcium channels with a rate proportional to the calcium current.

Decay of the free calcium level near the cell membrane is due to diffusion, buffering capacity of the cytoplasm as well as active transport and removal (see e.g. Hille 1984; Blaustein 1988). In the model, an exponential decay is used to describe these mechanisms. This results in the following equation for the intracellular calcium level, denoted $[Ca_{AP}]$:

$$\frac{d[Ca_{AP}]}{dt} = (E_{Ca} - E_{soma})\varrho_{AP} q^5 - \delta_{AP}[Ca_{AP}] \tag{13}$$

The two constants ϱ_{AP} and δ_{AP} are the rates of calcium ion influx and decay, respectively.

In many types of neurons, Ca^{2+} will activate Ca^{2+} dependent K^+ ($K_{(Ca)}$) channels (Hille 1984), which underlie the late phase of the afterhyperpolarization (AHP; see Fig. 3A; for lamprey, see Hill et al. 1985). In this model, the $K_{(Ca)}$ channels have a conductance proportional to the amount of Ca^{2+} in the Ca_{AP}-pool. This gives the following equation for the $K_{(Ca)}$ current:

$$I_{K(Ca)} = (E_K - E_{soma}) G_{K(Ca)} [Ca_{AP}] \tag{14}$$

The late AHP is a main factor involved in the spike frequency regulation in vertebrate neurons (Kernell and Sjöholm 1973; Baldissera and Gustafsson 1974). Without the late AHP, cells stimulated above threshold would tend to fire close to their maximum frequency without much of a dynamic range. With the late AHP, low stimulating currents can make the cell fire regularly at much lower frequencies, while fast spiking still occurs when larger currents are injected. The frequency regulation in a model neuron with a late AHP is shown in Fig. 3. The adaptation of firing frequency is evident in Fig. 3B (at 2 and 4 nA), where the first interspike interval is shorter than the following intervals due to subsequent summation of the late AHP's (cf. Baldissera and Gustafsson 1974). The current-frequency relation is shown in Fig. 3C. The curves for the first and second interspike intervals display a "primary range" at low intensities (below 1.5 nA and 2.5 nA, respectively) and a "secondary range" with a steeper slope at higher intensities of stimulation, as previously described e.g. for cat motoneurons (Baldissera and Gustafsson 1974; Kernell and Sjöholm 1973).

3 Synaptic communication

The main reason for using a multicompartment model for the dendritic tree is to make it possible to model

synapses at various distances from the soma on the postsynaptic cell. The passive model used also influences the choice of the synapse model. Since the transmission from one cell to another already includes several time-intergrating steps in a multicompartment model, a simple description of the time course of the postsynaptic response was found to be sufficient. The conventional synapse is modeled with a transmembrane conductance in the postsynaptic compartment. Following the initiation of the presynaptic spike, and after a delay which is individual for each synapse, the conductance is increased (Fig. 4A). The delay represents the time for an action potential to be propagated down the axon and the transsynaptic delay. The conductance remains high for a fixed length of time and then returns to zero.

The current entering the postsynaptic compartment then becomes:

$$I_{syn} = (E_{syn} - E)G_{syn}s \tag{15}$$

where s is the activation level of the postsynaptic channels, zero when the synapse is inactive and one when it is active. E is the membrane potential of the postsynaptic compartment, and E_{syn} is the reversal potential for the synaptic current involved.

For excitatory synapses, E_{syn} is typically set to 0 mV representing e.g. glutamate mediated transmission caused by Na^+ and K^+ ion flow (Fig. 4A). For inhibitory synapses, we have been using a reversal potential, E_{syn}, of -85 mV, being close to the equilibrium potential for Cl^- ions, corresponding e.g. to glycinergic transmission. The synaptic efficacy is determined both by the conductance G_{syn} and by the duration of the synaptic current.

Figure 4 illustrates examples of simulated postsynaptic potentials (PSP's) in the postsynaptic cell in a pair of connected model neurons. Note the different shapes of the EPSP's evoked by synaptic input to different dendritic compartments (Fig. 4B). Figure 5A shows the amplitude of an EPSP at different holding potentials.

3.1 NMDA receptor channels

Three different excitatory amino acid (EAA) receptors have been described: AMPA (quisqualate), kainate and N-methyl-D-aspartate (NMDA) receptors (Watkins and Evans 1981). The NMDA channel is unique in that it is not only dependent on the presence of a transmitter substance to open. At the resting membrane potential it is blocked by Mg^{2+} ions at physiological levels, but this block gradually disappears as the cell becomes depolarized. This gives the NMDA channel a pronounced voltage dependence (Ascher and Nowak 1988). When the NMDA-receptors are activated, a cell which be comes depolarized tends to stay depolarized, thus expressing a plateau property.

By introducing a variable p, a value between zero and one, for this Mg^{2+} block, we get the following expression for the synaptic current for an NMDA-receptor based synapse:

$$I_{NMDA} = (E_{NMDA} - E)G_{NMDA}ps \tag{16}$$

A similar formalism was chosen for this voltage dependent phenomenon as for the other voltage dependent channels, though the underlying mechanism is known to be quite different. The equations are the same as those used by Ascher and Nowak (1988; see also Neher and Steinbach 1978):

$$\frac{dp}{dt} = \alpha_p(1-p) - \beta_p p \tag{17}$$

$$\alpha_p = Ae^{E/C} \qquad \beta_p = Ae^{-E/C} \tag{18}$$

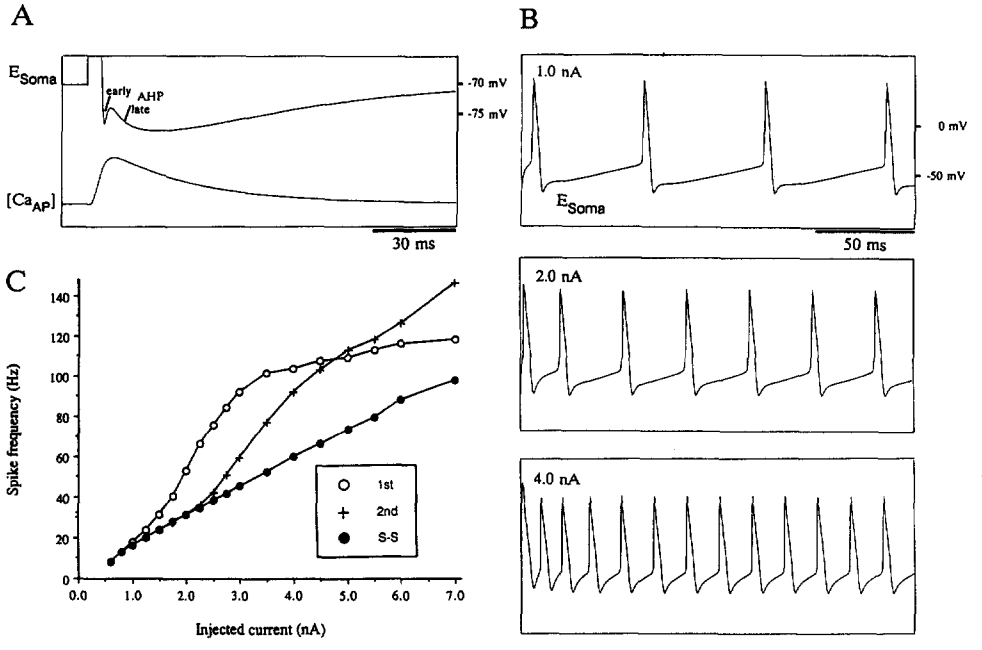

Fig. 3. A Spike with AHP and intracellular calcium concentration. The apparent mismatch in timing between the maxima of the late AHP and the $[Ca_{AP}]$ is due to a depolarizing effect from the dendritic compartments, influencing E_{soma}. **B** Repetitive firing as a result of intracellular tonic current injection showing the dynamic range of firing frequency, as well as spike frequency adaptation. **C** Current vs frequency (i.e. 1/interval) plot for the first and second interspike intervals, and for steady state firing (1st, 2nd, S-S, respectively)

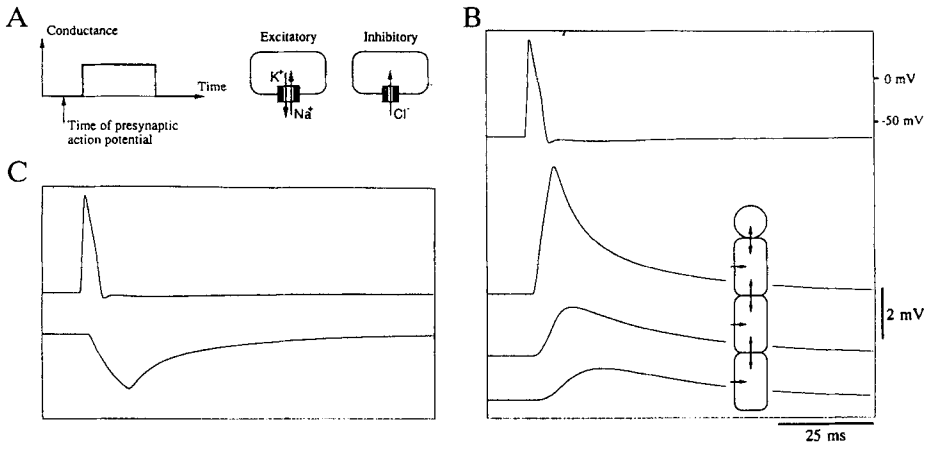

Fig. 4. **A** The mechanism used to simulate synaptic input. See text for details. **B** EPSP's as seen in the soma when receiving synaptic input on different dendritic compartments. **C** IPSP as seen in the soma from a synapse situated on the first dendritic compartment (duration of synaptic current was set longer than in **B**). Top trace in **B** and **C** is the presynaptic spike

Table 1. Parameters used in describing the ion channels

		Na^+		K^+	Ca^{2+}	NMDA
		m	*h*	*n*	*q*	*p*
α	*A* (mV^{-1} ms^{-1})	0.2	0.08	0.02	0.08	0.7 (ms^{-1})
	B (mV)	−40	−40	−31	−10	–
	C (mV)	1	1	0.8	11	17
β	*A* (mV^{-1} ms^{-1})	0.06	0.4 (ms^{-1})	0.005	0.001	0.1 (ms^{-1})
	B (mV)	−49	−36	−28	−10	–
	C (mV)	20	2	0.4	0.5	17

Table 2. Parameters used for the neuron simulations in this paper. The parameters correspond to those of excitatory interneurons in the simulations of the spinal locomotor network of the lamprey

Passive Properties		Active Properties			
E_{leak}	−70 mV	E_{Na}	50 mV	ϱ_{AP}	4 s^{-1} mV^{-1}
G_m Soma	0.003 μS	G_{Na}	1.0 μS	δ_{AP}	30 s^{-1}
C_m Soma	0.03 nF	E_K	−90 mV	ϱ_{NMDA}	0.5 s^{-1} mV^{-1}
G_m Dendrites	0.01 μS	G_K	0.2 μS	δ_{NMDA}	3 s^{-1}
C_m Dendrites	0.3 nF	E_{Ca}	150 mV	$G_{K(Ca)}$	0.01 μS
G_{core}	0.04 μS	G_{Ca}	0 μS		

In addition to its voltage dependence, another special property of the NMDA-receptor is that the associated channel is permeable not only to Na^+ and K^+ ions, but also to Ca^{2+} (Mayer et al. 1987). This does not influence the resulting current much (actually, the reversal potential for these synapses is set slightly above those for traditional excitatory synapses), but the main effect is that the inflow of Ca^{2+} ions will activate the $K_{(Ca)}$ channels of the cell. Ca^{2+} entering in this way can accumulate over seconds, thereby causing a gradual hyperpolarization of the cell until the NMDA channels become blocked due to their voltage dependence (Wallén and Grillner 1987). This mechanism is important for burst termination during slow swimming in the lamprey network (Grillner et al. 1991) and is therefore essential to reproduce in the simulations.

Because the time constants involved in this Ca^{2+} accumulation differ compared to those of the Ca_{AP}-pool, we have chosen to use two separate Ca^{2+} pools, both influencing the $K_{(Ca)}$ channels (cf. Brodin et al. 1991). For the Ca_{NMDA}-pool we get a differential equation similar to that of the Ca_{AP}-pool but with different

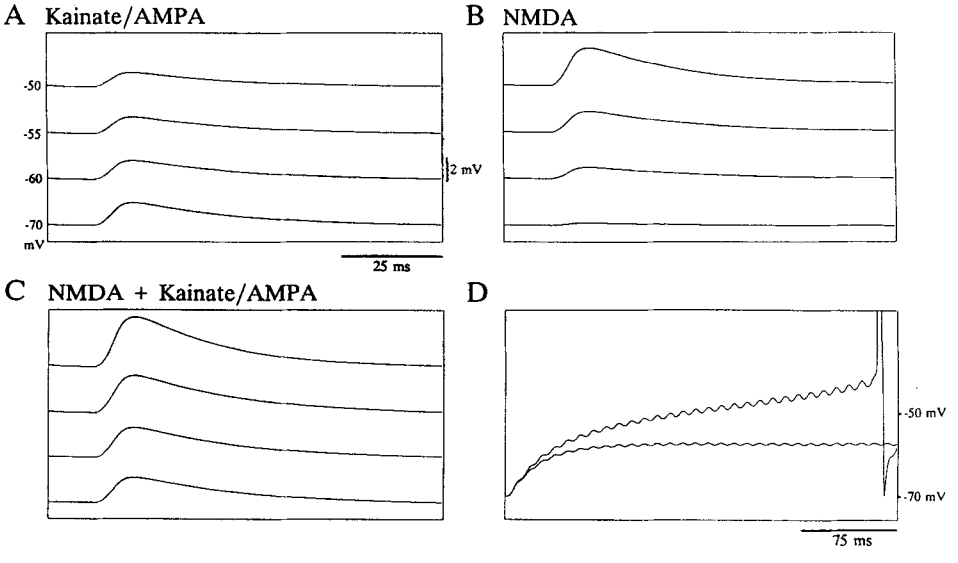

Fig. 5A–D. Comparison between simulated kainate/AMPA and NMDA receptor mediated EPSP's. **A** The "conventional" kainate/AMPA EPSP decreases in size with membrane depolarization. **B** The NMDA EPSP instead increases in size. **C** Simulation of the mixed kainate/AMPA – NMDA EPSP. **D** Temporal summation of synaptic input mediated by NMDA + kainate/AMPA receptors (*upper trace*; spike threshold is reached) and by kainate/AMPA receptors alone (*lower trace*)

values for the rate parameters (see Table 2):

$$\frac{d[Ca_{NMDA}]}{dt} = (E_{NMDA} - E)\varrho_{NMDA} ps - \delta_{NMDA}[Ca_{NMDA}] \quad (19)$$

The expression given above for the net current through the $K_{(Ca)}$ channels is thus extended to:

$$I_{K(Ca)} = (E_K - E)G_{K(Ca)}([Ca_{AP}] + [Ca_{NMDA}]) \quad (20)$$

Examples of NMDA-receptor mediated EPSP's are given in Fig. 5B. Note that at a hyperpolarized level (−70 mV) the NMDA channels are essentially blocked (Fig. 5B), while at more depolarized levels the NMDA-receptor mediated EPSP *increases* in size due to its voltage dependence, in contrast to the "conventional" kainate/AMPA EPSP's (Fig. 5A). Many synapses utilize both NMDA and kainate/AMPA receptors (Dale and Grillner 1986) as simulated in Fig. 5C. Note that the, as yet unexplained, difference in time course observed between the two types of EPSP's (e.g. Dale and Grillner 1986) was not accounted for in these simulations. The voltage dependence of the NMDA-receptor mediated EPSP has functional consequences for instance during temporal summation of synaptic input, as illustrated in Fig. 5D. A detailed description of the simulations of the NMDA-receptor induced membrane properties, including pacemaker-like behavior, is given separately (Brodin et al. 1991).

4 Computer simulation

The cell model as described above includes, in all, eleven state variables: the membrane potential E for the four compartments, the channel variables m, h, n, q, p, and the two calcium pool concentrations $[Ca_{AP}]$ and $[Ca_{NMDA}]$. Each of these variables is described by a corresponding ordinary first order differential equation and this set of eleven coupled equations constitutes the complete mathematical formulation of the model. Given some initial values for the state variables it is, in principle, possible to compute the values of the state variables for any time in the future. Such a complex set of equations is, however, impossible to solve analytically. Thus, computer based numerical methods must be applied.

4.1 Numerical methods

There exists a number of different numerical methods for solving such systems of coupled differential equations. These are all based on the technique of taking small timesteps and computing the changes of each state variable through the corresponding differential equation. This computation can not be exact due to the fact that the equations use the values of the state variables, all varying during the time step. By using smaller timesteps, the errors introduced can be made arbitrarily small, but the penalty is that the computational burden increases. Different numerical methods have been designed to circumvent this dilemma in various ways.

Which method is the most suited for a particular set of equations depends both on the properties of the equations and on the desired accuracy of the result. In our case, we have no need for a high numerical accuracy (at the inevitable cost of longer computational time). We would rather like to spend the computing resources on longer simulations and larger systems.

One important property of the system is that the time constants involved in the equations differ very much, for instance the sodium channel activation is very fast while the decay in the Ca_{NMDA}-pool is much slower. This indicates that a straightforward numerical method might run into problems with stability because of the stiffness of the system. A system is called stiff when the maximum step length that can be taken during the simulations is limited, not by the desired accuracy, but by the stability. If too large timesteps are taken we do not simply get a somewhat larger error, but the simulation "runs amok". This fact prevented us from taking advantage of our modest accuracy requirements by simply using longer timesteps.

These considerations led us to try some numerical methods designed especially for systems of stiff differential equations, along with standard methods, typically of the Runge–Kutta type (see e.g. Dahlquist and Björck 1974). Much larger timesteps could be taken with implicit methods designed for stiff systems and consequently, many of our simulations were done using these methods. The method used was primarily the colos method, a one-legged single step implicit method (Dahlquist G. and Littmarck S., personal communication). This method is, however, not suited for low-accuracy simulations at high speed. Such simulations have great advantages while tuning parameters because it gives a fast turnaround. For such simulations a different numerical method was used, utilizing the fact that all the equations can be written on the form:

$$\frac{dy}{dt} = yf(\ldots) + g(\ldots) \quad (21)$$

i.e. the corresponding state variable (y in this example) only occurs in a linear context on the right hand side. This makes it possible to perform an exponential prediction in each step. Using a fixed timestep h gives the next value as:

$$y_{t+h} = y_t + (e^{hf(\ldots)} - 1)\left(y_t + \frac{g(\ldots)}{f(\ldots)}\right) \quad (22)$$

When $f(\ldots)$ is zero, this reduces to:

$$y_{t+h} = y_t + hg(\ldots) \quad (23)$$

which is identical to a straightforward Euler method.

This technique, which has earlier been used by e.g. MacGregor and Lewis (1977) for neural simulations, has the advantage that much larger timesteps can be taken without any stability problems. However, there is no guarantee that the results are actually correct, but this can easily be checked by rerunning the simulations

with the final parameter values either with a smaller time step or with the colos method.

When simulating single neurons, much speed can be gained by the use of automatic regulation of the time step so that larger steps are taken when no fast events, typically action potentials, occur. However, when dealing with simulations of large sets of communicating cells, activity in any one of the cells will force the use of small steps. Thus, in a large enough system nothing will be gained from automatic time step regulation. One way to pursue this would be to use different time steps for different parts of the system but there are currently no established numerical methods to handle this.

4.2 Implementations

The model described in this paper has been implemented in two different programs. The first one is designed especially for fast turnaround while working with single cells and small networks and runs on the Macintosh II personal computer. The second one is designed to handle larger simulations running on UNIX based multiuser computers and full size workstations.

The Mac II program was initially designed for single cell simulations and then later extended to handle networks of up to about ten neurons. The design was made to promote "rapid prototyping", i.e. it should be easy to make changes in parameter values and then rerun the simulation, again and again. This is accomplished by a window-based user interface where the user has direct access to all relevant parameter values in a directly editable form. Running a simulation requires only a single key press and the result is presented as multiple graphs in a separate window, showing selected state variables.

In practice, the factor limiting the number of neurons that can be handled in the Mac II program is not only the actual capacity of the program, but rather the large set of parameters to be kept up to date. To avoid this problem to some extent, two extensions have been made. First, user defined variables were introduced, permitting the user to simply change the value of one variable instead of making many changes throughout the parameter list. These variables can also be used in arbitrary arithmetic expressions, which has proven most useful, e.g. when simulating the application of chemical agonists and antagonists as multiplicative factors in conductance parameters. Second, since most parameters are identical for all cells, a set of default parameter values can be defined and then only exceptions to these defaults have to be specified for each cell individually.

The UNIX implementation is designed to handle this complexity in a more general way by a set-based organization of parameters (Ekeberg et al. 1990). Parameter values are inherited, in much the same way as in modern object-oriented programming languages. This makes it possible to specify e.g. all Na^+ channel properties in one place and then make the individual neurons inherit these values with the possibility to modify them locally. This inheritance can occur in several steps making it useful for a natural hierarchical organization of cell populations, classes of synapses etc. The same inheritance scheme is also used for user defined variables which provides a powerful framework for describing e.g. experimental conditions.

5 Discussion

The model described has been designed primarily for the simulation of the neuronal circuitry generating locomotor rhythmicity in the lamprey. However, the general character of the model allows for the properties of several other types of neurons or networks to be reproduced, with appropriate parameter tuning. For example, in Fig. 6 the firing behavior of some different classes of neocortical neurons (Connors and Gutnick 1990) has been simulated using the present model (Fransén and Lansner 1990).

In terms of the number of parameters necessary to specify, the neuron model is quite complex. For instance, a neuron with three dendritic compartments requires the specification of approximately 60 parameter values. Furthermore, each synapse adds another seven values. A careful tuning of these parameter values is essential and has to be carried out in parallel with test simulations. During this process, corresponding biological data has to be taken into consideration so that parameter values are kept within physiological limits and the overall behavior of the model becomes biologically realistic.

Although the neuron simulations performed have yielded results that correspond well to experimental findings, there are certain properties that have not been explored in the present study, e.g. postinhibitory rebound. The contribution by such properties remains to be tested.

The model can easily be extended to include several other neuronal mechanisms of importance in a particular biological system. For instance, for some types of

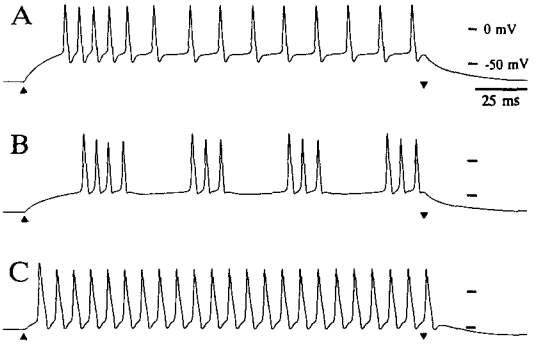

Fig. 6A–C. Three different types of neocortical neurons have been simulated using the current model. **A** A regular-spiking neuron showing a pronounced adaptation. **B** An intrinsically bursting neuron. **C** A general cortical cell firing at high frequency with a low threshold. Arrowheads indicate onset and termination of depolarizing DC-current injection

synapses, especially those with a long lasting effect, it might be necessary to include a graded decay of the conductance instead of an abrupt termination. There are also several types of synaptic mechanisms which have not yet been included. Several transmitters act on K^+ channels, which could be modeled in the same way as Cl^- mediated IPSP's. Synaptic effects on $K_{(Ca)}$ channels, such as those produced by 5-HT which influences the afterhyperpolarization, could also be simulated. Likewise, mechanisms for presynaptic modulation could be included, as well as non-synaptic mechanisms for neuronal interaction, such as an increase in extracellular potassium. In the present simulations, the ion channels underlying the action potential are located in the soma compartment, while the transmitter-gated, postsynaptic channels are placed on different dendritic compartments. The model allows, however, the localization of any channel to be altered.

There are also several ways in which the model could be simplified without violating its realistic nature, resulting in more efficient simulations. When simulating large sets of neurons, the actual shape of the individual action potentials may be of minor importance. This is in contrast to the fact that most of the simulation time is spent on computing them. Under some conditions it might be advantageous to handle the action potentials separately and to use differential equations only for slower phenomena, thus making the simulations run significantly faster. In addition, the time delay of the Mg^{2+} block of NMDA channels may not be necessary, and if so, the model of the voltage dependence could be simplified to a sigmoid shaped function.

Further simplification of the realistic neuron model described here gives possibilities to approach the abstract models of neural networks. This could include the reduction to one single compartment and even replacing the action potential output with a value representing firing frequency. By doing simplifications gradually, this becomes a way to bridge the gap between the study of real neural systems and of artificial neural network models. This will, hopefully, prove to be mutually beneficial for both research areas.

6 Conclusions

A mathematical model of the single neuron and the synaptic interaction has been presented. The level of complexity of the model has been chosen so that experimental cell data can be interpreted in terms of the model while the resulting behavior of a network can be studied by computer simulation. By tuning parameters it is possible to make this model mimic many different types of neurons.

Simulations of large sets of neurons require, for practical reasons, fast numerical methods. Different methods have been investigated for computer simulation of the resulting system of coupled differential equations. Two of these have proven suitable: one implicit method for highly accurate simulations and one using exponential prediction for faster test simulations. Two different implementations of the model have been made, one with emphasis on fast user interaction for small networks and another designed for larger systems.

The described computer simulation model of the neuron and of the synaptic interaction has proven very useful in the analysis of the segmental network for locomotion in the lamprey. Not only has it been possible to simulate the rhythm generating capability of the network and to simulate and test the role of NMDA receptor activation (Grillner et al. 1991, and unpublished; Brodin et al. 1991; cf. also Grillner et al. 1988, 1989); the key mechanisms thought to be involved in the supraspinal and sensory control of the network, have also been successfully simulated and tested (Lansner et al. 1989; Grillner et al. 1991). The analyzing power of realistic computer simulations in the study of the lamprey locomotor network and its control is apparent. The simulations have given several new insights into the functioning of this motor system. It is obvious that this could not have been achieved without computer modeling.

Acknowledgement. This work was supported by the Swedish Natural Science Research Council (proj. no. B-TV-3531-100) and the Swedish National Board for Technical Development (proj. no. 90-02759).

References

Anderson JA, Rosenfeld E (1988) Neurocomputing. Foundations of research. MIT Press, Cambridge, Mass

Ascher P, Nowak L (1988) The role of divalent cations in the N-methyl-D-aspartate responses of mouse central neurones in culture. J Physiol 399:247–266

Baldissera F, Gustafsson B (1974) Firing behaviour of a neurone model based on the afterhyperpolarization conductance time course and algebraical summation. Adaptation and steady state firing. Acta Physiol Scand 92:27–47

Blaustein MP (1988) Calcium transport and buffering in neurons. Trends Neurosci 11:438–443

Brodin L, Tråvén H, Lansner A, Wallén P, Ekeberg Ö, Grillner S (1991) Computer simulation of N-methyl-D-aspartate (NMDA) receptor induced membrane properties in a neuron model. J Neurophysiol (in press)

Buchanan JT, Grillner S (1987) Newly identified 'glutamate interneurons' and their role in locomotion in the lamprey spinal cord. Science 236:312–314

Connors WB, Gutnick MJ (1990) Intrinsic firing patterns of diverse neocortical neurons. Trends Neurosci 13:99–104

Dahlquist G, Björck Å (1974) Numerical methods. Prentice Hall, Englewood Cliffs NJ

Dale N, Grillner S (1986) Dual-component synaptic potentials in the lamprey mediated by excitatory amino acid receptors. J Neurosci 6:2653–2661

Edman Å, Gestrelius S, Grampp W (1987a) Analysis of gated membrane currents and mechanisms of firing control in the rapidly adapting lobster stretch receptor neurone. J Physiol 385: 649–669

Edman Å, Gestrelius S, Grampp W (1987b) Current activation by membrane hyperpolarization in the slowly adapting lobster stretch receptor neurone. J Physiol 385:671–690

Ekeberg Ö, Stensmo M, Lansner A (1990) SWIM – a simulator for real neural networks. Tech Rep TRITA-NA-9014, Royal Institute of Technology, Stockholm

Frankenhaeuser B, Huxley AF (1964) The action potential in the myelinated nerve fibre of *Xenopus Laevis* as computed on the basis of voltage clamp data. J Physiol 171:302–315

Fransén E, Lansner A (1990) Modelling Hebbian cell assemblies comprised of cortical neurons. Proc Open Network Conference

on Neural Mechanisms of Learning and Memory, London 3–6 April 1990, p 4:9
Getting PA (1989) Emerging principles governing the operation of neural networks. Ann Rev Neurosci 12:185–204
Grillner S, Wallén P, Dale N, Brodin L, Buchanan JT, Hill R (1987) Transmitters, membrane properties and network circuitry in the control of locomotion in lamprey. Trends Neurosci 10: 34–41
Grillner S, Buchanan JT, Lansner A (1988) Simulations of the segmental burst generating network for locomotion in lamprey. Neurosci Lett 89:31–35
Grillner S, Christenson J, Brodin L, Wallén P, Hill R, Lansner A, Ekeberg Ö (1989) Locomotor system in lamprey: neural mechanisms controlling spinal rhythm generation. In: Jacklet JW (ed) Neural and cellular oscillators, Dekker, New York, pp 407–434
Grillner S, Wallén P, Brodin L, Lansner A (1991) Neuronal network generating locomotor behavior in lamprey: circuitry, transmitters, membrane properties and simulations. Ann Rev Neurosci 14:169–199
Hill RH, Åhrem P, Grillner S (1985) Ionic mechanisms of 3 types of functionally different neurons in the lamprey spinal cord. Brain Res 358:40–52
Hill RH, Brodin L, Grillner S (1989) Activation of N-methyl-D-aspartate (NMDA) receptors augments repolarizing responses in lamprey spinal neurons. Brain Res 499:388–392
Hille B (1984) Ionic channels of excitable membranes. Sinauer, Sunderland, Mass
Hodgkin AL, Huxley AF (1952) A quantitative description of membrane current and its application to conduction and excitation in nerve. J Physiol 117:500–544
Holden AV (1980) Autorhythmicity and entrainment in excitable membranes. Biol Cybern 38:1–8
Kernell D, Sjöholm H (1972) Motoneurone models based on 'voltage clamp equations' for peripheral nerve. Acta Physiol Scand 86:546–562
Kernell D, Sjöholm H (1973) Repetitive impulse firing: comparisons between neurone models based on 'voltage clamp equations' and spinal motoneurones. Acta Physiol Scand 87:40–56
Koch C, Segev I (1989) Methods in neuronal modeling, from synapses to networks. MIT Press, Cambridge, Mass
Lansner A (1982) Information processing in a network of model neurons. A computer simulation study. Tech Rep. TRITA-NA-8211, Dept. of Numerical Analysis and Computing Science, The Royal Institute of Technology, Stockholm
Lansner A, Ekeberg Ö (1985) Reliability and speed of recall in an associative network. IEEE Trans PAMI 7:490–498
Lansner A, Ekeberg Ö (1989) A one-layer feedback artificial neural network with a Bayesian learning rule. Int J Neural Sys 1:77–87
Lansner A, Ekeberg Ö, Tråvén H, Brodin L, Wallén P, Stensmo M, Grillner S (1989) Simulation of the experimentally established segmental, supraspinal and sensory circuitry underlying locomotion in lamprey. Soc Neurosci (abstr) 15:1049
Lippmann RP (1987) An introduction to computing with neural nets. IEEE ASSP Mag April:4–22
MacGregor RJ (1987) Neural and brain modeling. Academic Press, New York
MacGregor RJ, Lewis ER (1977) Neural modeling. Electrical signal processing in the nervous system. Plenum Press, New York
MacGregor RJ, Oliver RM (1974) A model for repetitive firing in neurons. Kybernetik 16:53–64
Mayer ML, MacDermott AB, Westbrook GL, Smith SJ, Barker JL (1987) Agonist- and voltage gated calcium entry in cultured mouse spinal cord neurons under voltage clamp measured using arsenazo III. J Neurosci 7:3230–3244
Mulloney B, Perkel DH (1988) In: Cohen AH, Grillner S, Rossignol S (eds) Neural control of rhythmic movements in vertebrates. Wiley, pp 415–453
Neher E, Steinbach JH (1978) Local anaesthetics transiently block currents through single acetylcholine-receptor channels. J Physiol 277:153–176
Perkel DH (1976) A computer program for simulating a network of interacting neurons. Comput Biomed Res 9:31–74
Rall W (1977) Core conductor theory and cable properties of neurons. In: Brookhart JM, Mountcastle VB, Kandel ER (eds) Handbook of physiology, Sect. 1, vol 1(1). Am Physiol Soc 39–97
Roberts A, Tunstall MJ (1990) Mutual re-excitation with post-inhibitory rebound: a simulation study on the mechanisms for locomotor rhythm generation in the spinal cord of *Xenopus* embryos. Eur J Neurosci 2:11–23
Rumelhart DE, McClelland JL (1986) Parallel distributed processing. Explorations in the microstructures of cognition. MIT Press, Cambridge Mass
Stein RB (1965) A theoretical analysis of neuronal variability. Biophys J 5:173–194
Traub RD, Llinas R (1977) The spatial distribution of ionic conductances in normal and axotomized motorneurons. J. Neurosci 2:829–849
Tsien RW (1983) Calcium channels in excitable cell membranes. Ann Rev Physiol 45:341–358
Tsien RW, Lipscombe D, Madison DV, Bley KR, Fox AP (1988) Multiple types of neuronal calcium channels and their selective modulation. Trends Neurosci 11:431–438
Wallén P, Grillner S (1987) N-methyl-D-aspartate receptor-induced, inherent oscillatory activity in neurons active during fictive locomotion in the lamprey. J Neurosci 7:2745–2755
Wallöe L (1968) Transfer of signals through a second order sensory neuron. Universitesforlagets Trykningssentral, Oslo
Watkins JC, Evans RH (1981) Excitatory amino acid transmitters. Ann Rev Pharmacol Toxicol 21:165–205

Örjan Ekeberg
Department of Numerical Analysis and Computing Science
Royal Institute of Technology
S-100 44 Stockholm
Sweden